Histol Histopathol (2025) 40: 669-678

Histology and Histopathology
From Cell Biology to Tissue Engineering

ORIGINAL ARTICLE Open Access

The effectiveness of edible bird's nest in lowering VEGF, CD31, and PDGFR-β levels in diabetic retinopathy in rats with type 1 diabetes

Manaras Komolkriengkrai[1], Udomlak Matsathit[2], Nualpun Sirinupong[3] and Wipapan Khimmaktong[1]

[1]Department of Anatomy, Division of Health and Applied Sciences, Faculty of Science, Prince of Songkla University, Songkla, [2]Department of Food Science and Nutrition, Faculty of Science and Technology, Prince of Songkla University, Pattani and [3]Faculty of Agro-Industry, Prince of Songkla University, Hat Yai, Songkhla, Thailand

Summary. Aims. Diabetic eye disease, known as diabetic retinopathy (DR), is one of the problems that can arise from having high blood sugar for an extended period. This study aimed to investigate the effect of the edible bird's nest (EBN) on retinal angiogenesis in diabetic rats.

Methods. The 50 rats were separated into five different groups, each containing 10 rats: control, diabetes (DM), bird's nest-fed diabetes (75 mg/kg Body weight; BW), (EBN 75), (150 mg/kg BW) (EBN 150), and glyburide (GR) for an eight-week study. H&E and Masson's trichrome staining were utilized to investigate the retinal tissue and vascular changes. The immunofluorescence study was used to detect angiogenic protein expression. The vascular corrosion cast/SEM method was also used to evaluate capillary plexus formation within the retinal layer.

Results. From histological studies, DM rats have thinning of the retinal layer. Remarkably, the retinal vessels displayed dilations resembling ruptured blood vessels. The expression of vascular endothelial growth factor (VEGF) (30.51±2.62), cluster of differentiation 31 (CD31) (28.18±0.22), and platelet-derived growth factor receptor beta (PDGFR-β) (141.67±0.97) were increased. EBN 75 exhibited some small improvements in their blood vessels and eye tissue. At a dose of 150 mg/kg BW, EBN proved to be more effective. There was a significant decrease in VEGF and CD31 expression compared with the diabetic group ($p<0.001$ and $p<0.01$, respectively).

Conclusions. These studies have demonstrated that EBN can lower the growth levels of VEGF, CD31, and PDGFR-β, which results in a decrease in angiogenesis and a recovery from a variety of diabetic retinopathy-related diseases.

Key words: Edible bird's nest, Blood vessels, Angiogenesis, Retina, Diabetic retinopathy

Corresponding Author: Wipapan Khimmaktong, Department of Anatomy, Division of Health and Applied Sciences, Faculty of Science, Prince of Songkla University, Songkhla, 90110 Thailand. e-mail: wipapan.k@psu.ac.th

www.hh.um.es. DOI: 10.14670/HH-18-825

Introduction

Diabetes mellitus (DM) stands as a persistent global metabolic disorder, ranking as the fourth leading contributor to global mortality due to its intricate associations with various complications within the microvasculature (Roden, 2016). These complications materialize because of the expansion and dysfunction of small blood vessels. The prevalence of DM is on an alarming rise worldwide, affecting individuals across age groups, including adolescents and children, in both developed and developing nations. This growing trend poses a substantial health challenge, imparting significant burdens on public health systems and giving rise to a spectrum of related health concerns (Park and Roh, 2016). Diabetic retinopathy (DR) emerges as a challenging medical condition characterized by the irreversible loss of vision in individuals with poorly managed elevated blood glucose levels (Klein, 2007).

The interplay between persistent hyperglycemia and the intricate vasculature of various organs forms the bedrock of diabetic complications. The eyes, being endowed with a delicate and intricate network of blood vessels, are particularly susceptible to these complications (Wang and Lo, 2018). DR, a complication of DM, has emerged as a significant contributor to visual impairment and blindness, posing substantial challenges to healthcare systems and quality of life for affected individuals (Klein, 2007). It has been known for a long time that DR is a microvascular disease. It is generally agreed that hyperglycemia is a significant contributor to the pathophysiology of retinal microvascular injury.

Several metabolic processes, such as the polyol route, the buildup of advanced glycation products (AGEs), the protein kinase C (PKC) pathway, and the hexosamine pathway, have been linked to the hyperglycemia-induced damage to the cardiovascular system (Brownlee, 2005). While hyperglycemia is responsible for the production of free radicals, it also reduces the effectiveness of the endogenous antioxidant defense system in diabetic patients (Pitocco et al., 2010).

The production of edible bird's nest (EBN) is a fascinating process involving the collection of the saliva of swiftlets, who make their homes in limestone caves. For centuries, this remarkable substance has been an integral part of Chinese culinary traditions, notably in the creation of dishes like bird's nest soup. With a history spanning over 1,200 years, its consumption has been associated with the potential to elevate energy levels, counteract the effects of aging, and promote holistic health (Ma and Liu, 2012). EBN boasts a high safety threshold, with a lethal dose (LD50) exceeding 5,000 mg/kg. As per the globally harmonized classification system (GHS), it falls within the secure Category 5 or unclassified range. This underscores its suitability for human consumption without safety concerns (Haghani et al., 2016). EBN is a traditional food supplement from Asia that is well-known for its nutritional content. It has been demonstrated in several studies to be an excellent source of antioxidants, with anti-inflammatory properties (Choy et al., 2021). EBN treatment significantly ameliorated pathological changes and increased the protein expression of insulin and glucose transporters in pancreatic islets (GLUT-2), liver, and skeletal muscle (GLUT-4). There is a significant concentration of sialic acid in EBN, and this may play a role in the development of the brain and learning capacity (Oliveros et al., 2018). An exogenous supplement of sialic acid reduced the severity of atherosclerosis in mice with apolipoprotein E deficiency. This was accomplished in part by increasing antioxidant activity, which was archived by either restoring the activity of antioxidant enzymes or improving their protein expression. This led to the demonstration of the beneficial effect of sialic acid on cardiovascular disease (Guo et al., 2016).

This study delves into the impact of hyperglycemia on retinal vasculature and explores potential interventions to alleviate its adverse effects. By utilizing an experimental rat model of diabetes and examining the effects of EBN, this research aimed to shed light on the intricate molecular mechanisms that underlie DR. This comprehensive investigation encompassing histological, immunofluorescence, and vascular corrosion casting techniques offers insights into the cellular, molecular, and structural changes occurring in the retinal microenvironment in response to diabetes and potential interventions.

In essence, this study bridges the gap between hyperglycemia, retinal vasculature, and potential interventions, offering insights that could contribute to the development of strategies for preventing or managing DR. This study aimed to investigate the effect of EBN on retinal angiogenesis in diabetic rats. Understanding the complex interplay between hyperglycemia and retinal microvasculature is crucial for devising effective therapeutic approaches and improving the quality of life for individuals affected by diabetes-induced ocular complications.

Materials and methods

EBN extract preparation.

The cleaned and dried EBN was obtained from Nakhon Si Thammarat, Thailand. To obtain EBN water extract powder, the EBN extract was prepared with slight modifications from Careena et al. (2018) and Yew et al. (2014). EBN was weighed and crushed to powder by a dry grinding machine. The powder was soaked in distilled water at a ratio of 1:40 (w/v) for 24h at 4°C. The softened EBN was put into a stewing pot stewed at 95-98°C for 8-9h until EBN was fully dissolved. During stewing, the solution was gently stirred with a magnetic stirrer. Next, the homogenous solution was cooled and lyophilized by freeze-drying. The EBN extract powder obtained was aliquoted and kept at -20°C for further experiments.

Animals

The experimental procedures outlined in this study underwent thorough review and received approval from the Animal Ethics Committee at Prince of Songkla University, located in Songkhla, Thailand. For this research, a total of 50 male Wistar rats were selected, with a weight range of 200 to 250 grams and aged eight weeks. These rats were procured from Nomura Siam International Co., Ltd. The animals were provided with optimal living conditions within the laboratory setting, adhering to a 12-hour light-dark cycle. The environment was maintained with appropriate lighting, a controlled temperature of 25±2°C, and the lights were set to turn on at 7:00 a.m. Furthermore, the humidity level was maintained at 50±10%, and effective ventilation was ensured, creating a hygienic and conducive setting. They were fed *ad libitum* with standard rat chow containing protein, carbohydrates, fat, vitamins, and minerals.

Induction and assessment of diabetes

To induce diabetes in the rats, an intraperitoneal injection of a single dose of streptozotocin (STZ) [60 mg/kg body weight (BW); Sigma Aldrich; Merck KGaA] dissolved in 0.1 M citrate buffer (pH 4.5) was administered. The control rats received a single dose of 0.1 M citrate buffer alone. Rats with blood sugar levels exceeding 250 mg/dl were identified as diabetic (Komolkriengkrai et al., 2019). Blood sugar levels

from the lateral tail vein were analyzed using a blood glucose meter (AccuChek Active meter and test strips, Roche Diagnostics). Three days after the final STZ injection, the control and diabetic rats were randomly allocated into five groups: the 'C' group comprised normal control rats that received a balanced standard diet (n=10); the 'DM' group consisted of diabetic rats that received a balanced standard diet (n=10); the 'EBN75' group involved diabetic rats supplemented with 75 mg/kg BW of EBN along with a balanced standard diet (n=10); the 'EBN150' group included diabetic rats supplemented with 150 mg/kg BW of EBN along with a balanced standard diet (n=10); and the 'GR' group included diabetic rats treated with 4 mg/kg BW of glyburide in a 0.5 ml solution of 0.5% Tween-80 (n=20) (Wu et al., 2013). The rats were weighed, and clinical observations were conducted weekly. Blood glucose measurements were taken once a week at the week's end for a total of eight weeks. The first week of measurement commenced seven days after the experiment's initiation (end of the week). Consequently, substances or drugs were administered for a week before blood sugar measurements were taken, resulting in distinct blood sugar values among the groups by the first week's conclusion. Following the sacrifice of the experimental rats, tissue samples were collected. Within each group, half of the rats' tissues were subjected to H&E staining, Masson's trichrome staining, and immunofluorescence studies. The other half of the rats in each group underwent resin injection for vascular corrosion casting, followed by scanning electron microscopy for analysis. To ensure ethical treatment, the experimental rats were euthanized using an excessive dose of thiopental (150 mg/kg; intraperitoneal injection). Death was confirmed by observing cardiac and respiratory arrest or fixed and dilated pupils. Blood sugar levels were assessed by the Southern Lab Center at Saha Clinic (using a Siemens ADVIA 1800 System Analyzer; Siemens Healthineers).

Histological preparation for H&E and Masson's trichrome staining

For histological analysis, eyes from all groups were carefully dissected and promptly immersed in 10% formalin for six hours at room temperature. The tissue sections underwent dehydration through a decreasing ethanol sequence (70, 80, 90, 95, and 100%), each stage lasting one hour and being performed twice consecutively. After the dehydration steps, the samples underwent washing with a clearing agent, xylene, at room temperature, with each wash lasting 30 minutes. Following this, the tissue samples embedded in paraffin wax were sectioned into 5-µm slices. These sections were then subjected to staining using H&E and Masson's trichrome staining methods. All sections were meticulously examined and captured using an Olympus light microscope (BX-50, Olympus, Japan).

Immunohistochemistry and immunofluorescence analysis

Five-µm slices were cut from eye tissues fixed in paraffin. Following the deparaffinization of the sections in xylene, the sections were hydrated in gradient ethanol. A 30-minute permeabilization process was performed on the slides using PBST (phosphate-buffered saline; PBS with 0.1 Triton X-100). A blocking treatment was carried out by utilizing blocking serum in PBS for one hour at room temperature. Subsequently, an anti-PDGFR-β antibody (1:200, Abcam, Cambridge, UK) was incubated at a temperature of 4°C overnight. The sections were subjected to biotinylated anti-rabbit antibody (VECTASTAIN Elite ABC kit, Vector Laboratories Inc.), in blocking solution for two hours at room temperature. The slides were washed in PBS, then incubated with 3'-3' diaminobenzidine tetrachloride (Sigma-Aldrich; Merck KGaA) as the substrate, and then counter-stained with hematoxylin.

To evaluate the quantities of vascular endothelial growth factor (VEGF) and CD 31, the eye underwent deparaffinization using xylene, followed by hydration, and then permeabilization using PBST for 30 minutes. Blocking was performed with horse serum in PBS for one hour at room temperature. This was followed by incubation with rabbit anti-VEGF (1:200; Abcam, Cambridge, MA, USA.) and mouse anti-CD 31 antibodies (1:200, Cell Signaling Technology). The sections were then exposed to the Vectafluor duet immunofluorescence double labeling kit (DK 8828; Abcam, Cambridge, MA, USA.) for 30 minutes at room temperature to identify VEGF and CD 31. The sections were mounted with VECTASHIELD® HardSet™ Antifade Mounting Medium with DAPI (Vector Laboratories, Inc.). The resulting images were observed and captured using a fluorescence microscope (Olympus D73 equipped with CellSens software). The percentage cell expression of VEGF and CD 31 was calculated utilizing the National Institutes of Health (NIH) ImageJ software version 1.52, which measured the fluorescence intensity.

Vascular corrosion cast technique/Scanning electron microscope.

The pre-casting procedure involved an intravascular injection of 0.5 ml of heparin solution (5,000 IU/ml), swiftly administered into the left ventricle to prevent blood clotting. A subsequent injection of around 400-500 ml of normal saline solution was carried out to completely remove all blood from the vascular system. Following this, Batson's no. 17 plastic mixture was promptly introduced into the cannula and directed through the ascending aorta until the backflow from venous vessels became observable. Each animal was then allowed to rest at room temperature, facilitating the settling of the casting medium.

The eyes were excised and immersed in warm water at 80°C to ensure the completion of the hardening process. Subsequently, the eye underwent a corrosive treatment in a 10% KOH solution at room temperature. Once the tissues were cleared, they were thoroughly washed in tap water and subsequently rinsed multiple times with distilled water. The resulting vascular cast of the eye was dissected under a stereomicroscope, yielding small specimens that were allowed to air dry. These specimens were then prepared for scanning electron microscopy (SEM) observation using a JEOL JSM-5400 device at an accelerating voltage of 10-15 KV.

Statistical analysis

The outcomes are presented as means plus the standard error of the mean. Statistical analysis was executed employing ANOVA, succeeded by the Bonferroni *post-hoc* examination. A *p*-value below 0.05 was regarded as indicative of a statistically significant distinction.

Results

Effect of edible bird's nest on blood glucose levels

After conducting the experimental study for eight weeks, the rats in the DM, EBN75, EBN150, and GR groups had significantly higher blood sugar levels compared with the control group ($p<0.0001$) (Fig. 1). Additionally, when rats received EBN at the dose of 75, 150 mg/kg BW, or glyburide, there was a substantial impact on lowering blood sugar levels. However, the EBN150 group exhibited significantly lower blood sugar levels ($p<0.01$, $p<0.001$, and $p<0.05$) at weeks 4-5, 6-7, and 8, respectively, when compared with DM rats.

The GR group exhibited significantly lower blood sugar levels ($p<0.01$) at weeks 3 and 5 and ($p<0.001$) at weeks 4, 6-7, and ($p<0.05$) at week 8 compared with DM rats (Fig. 1).

Histological observation of the retina

The investigation of retinal tissues is prompted by the essential role of retinal blood vessels in supplying nutrients and oxygen. Therefore, this study delved into the histopathological changes occurring within the retinal vasculature, cellular components, and layers of the retina. The analysis was conducted using a light microscope set at various magnifications, with a specific focus on the blood vessel wall.

The control group, which was maintained on a regular diet for eight weeks, exhibited unaltered retinal histology in both the retinal layers and blood vessels when subjected to H&E (Fig. 2A) and Masson's trichrome staining (Fig. 3A). Conversely, the DM group (Figs. 2B, 3B), had hyperglycemia induced by a single STZ administration (60 mg/kg BW) and subjected to eight weeks of observation, displayed distinct pathological characteristics. Particularly from H&E staining, a noticeable reduction in the thickness of the retinal ganglion cell layer was observed. Furthermore, significant changes included a visible thinning of the retinal layer and a distinct thickening of the inner limiting membrane (basement membrane). Remarkably, the retinal arterioles displayed dilations resembling ruptured blood vessels (Fig. 2B). Some arterioles exhibited a constricted lumen, accompanied by a thickened wall due to collagen fiber accumulation, which resulted in compromised vascular flexibility. This phenomenon was observable in Masson's trichrome-stained samples (Fig. 3B), where the blue-stained collagen fibers were concentrated around the blood vessel walls. Notably, hemorrhages were dispersed throughout the retinal layers. Furthermore, degeneration of bipolar and ganglion cells was also detected.

Of significant interest, the treatment groups EBN75 (Figs. 2C, 3C), EBN150 (Figs. 2D, 3D), and GR (Figs. 2E, 3E) displayed intriguing trends in ameliorating retinal thickness. Notably, EBN150-treated subjects demonstrated substantial improvement in retinal microstructural changes, closely resembling the control group. These observations suggest the potential of these interventions in mitigating the progression of DR by

Table 1. The mean expression levels of CD31 and VEGF protein within the retinal vascular walls through Immunofluorescence technique across each experimental rat group.

Group	Mean Intensity of Retina (pixel)	
	CD31	VEGF
C	14.42±0.64	15.66±1.60
DM	28.18±0.22*	30.51±2.62**
EBN75	26.10±0.59*	28.69±0.78**
EBN150	19.84±0.83$^{\#}$	21.77±1.17$^{\#\#}$
GR	17.10±0.71$^{\#}$	18.02±1.45$^{\#\#}$

Data are presented as mean ± SEM, *$p<0.0001$, *$p<0.01$ compared with group C, $^{\#}p<0.001$, $^{\#\#}p<0.01$ compared with group DM

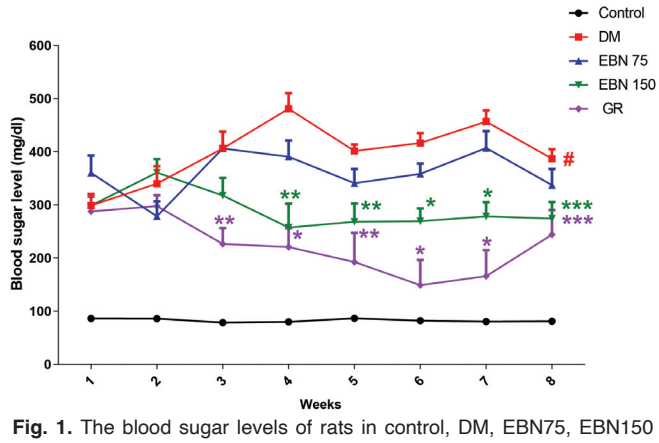

Fig. 1. The blood sugar levels of rats in control, DM, EBN75, EBN150 and GR groups for a period of 8 weeks. Values are mean ± SE, $^{\#}p<0.0001$ in DM, EBN75, EBN 150 and GR compared with the control rats. ***$p<0.05$, **$p<0.01$ and *$p<0.001$ in EBN 150 and GR compared with the DM rats.

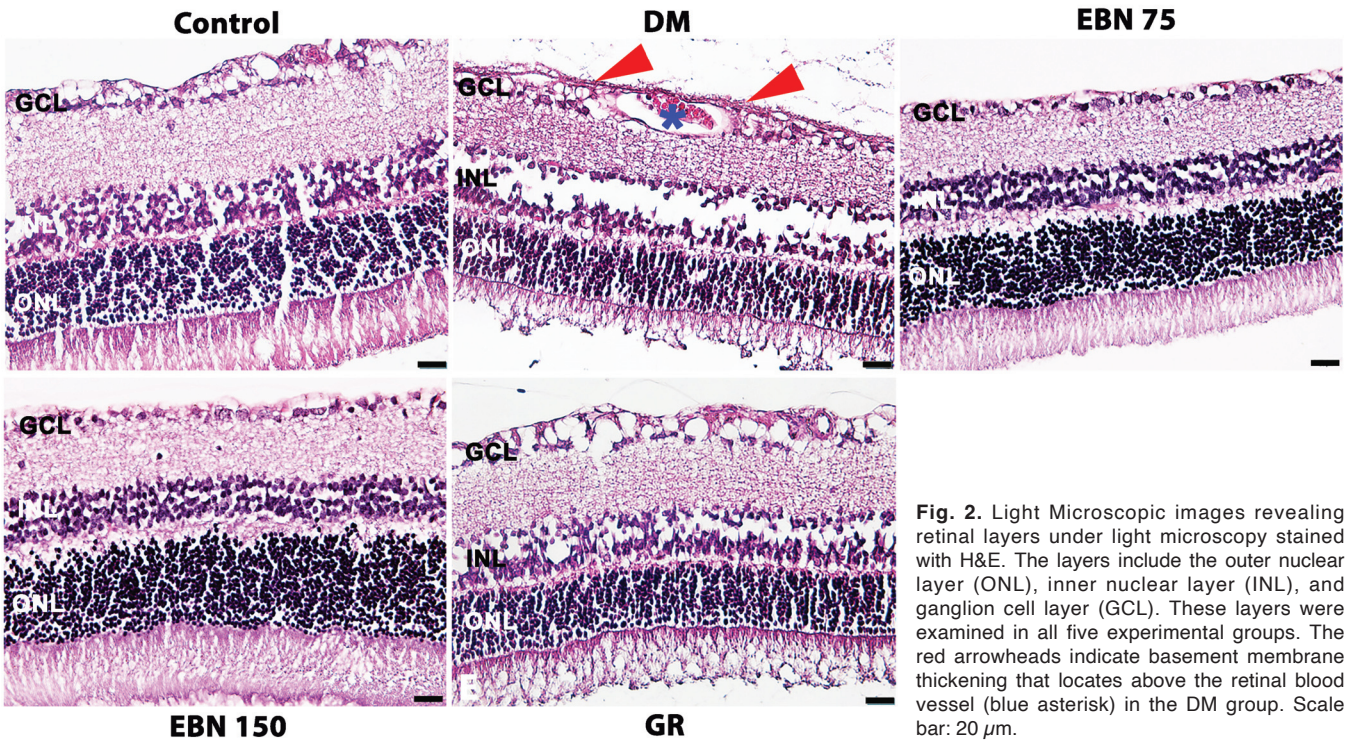

Fig. 2. Light Microscopic images revealing retinal layers under light microscopy stained with H&E. The layers include the outer nuclear layer (ONL), inner nuclear layer (INL), and ganglion cell layer (GCL). These layers were examined in all five experimental groups. The red arrowheads indicate basement membrane thickening that locates above the retinal blood vessel (blue asterisk) in the DM group. Scale bar: 20 μm.

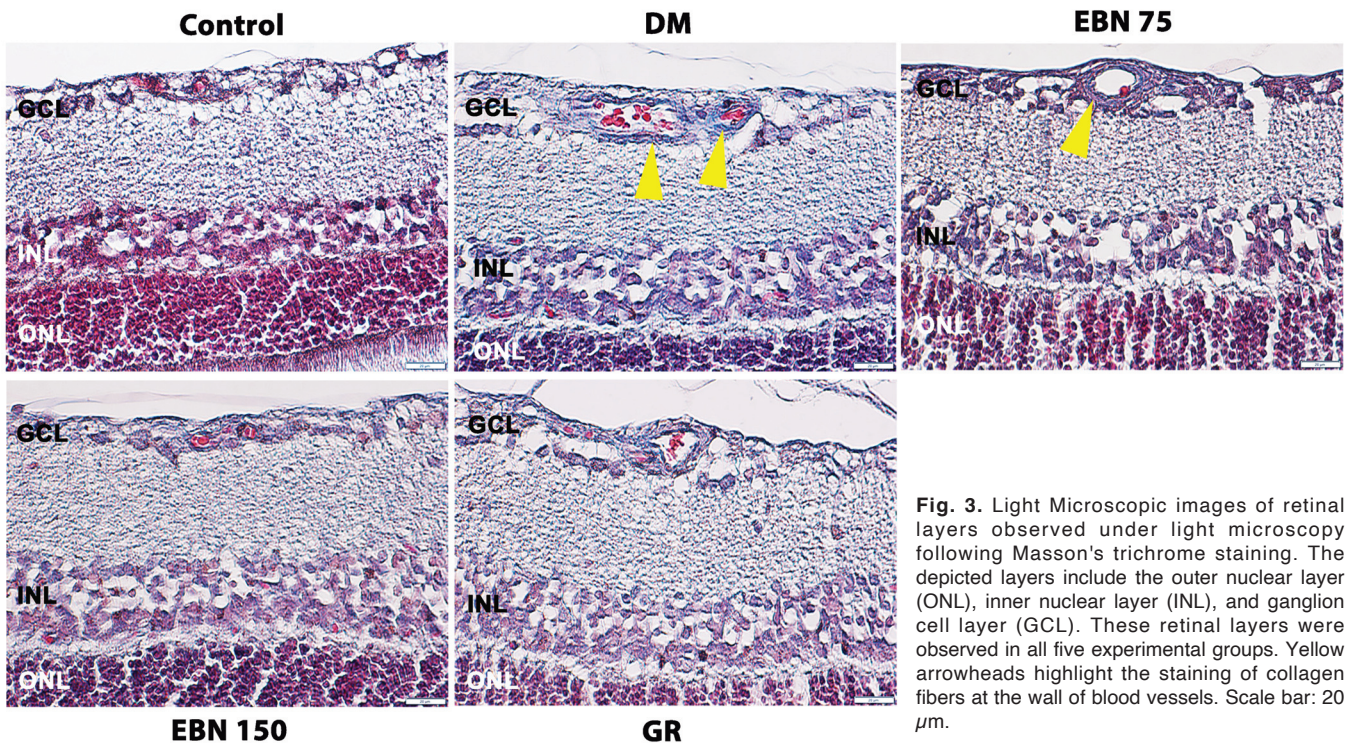

Fig. 3. Light Microscopic images of retinal layers observed under light microscopy following Masson's trichrome staining. The depicted layers include the outer nuclear layer (ONL), inner nuclear layer (INL), and ganglion cell layer (GCL). These retinal layers were observed in all five experimental groups. Yellow arrowheads highlight the staining of collagen fibers at the wall of blood vessels. Scale bar: 20 μm.

preserving retinal microvascular architecture and cellular integrity.

Analysis of immunofluorescence staining for VEGF and CD31

From the investigation of cluster of differentiation 31 (CD31) protein expression at the retinal layers in rats using the immunofluorescence technique, it was observed that CD31 protein expression in the retinal layers of the experimental group with induced DM exhibited increased levels compared with the control group, particularly in the distinct visualization of CD31 expression along the blood vessel walls within the retina (Fig. 4). The average intensity of CD31 protein fluorescence in the retinal layers of the DM group was 28.18±0.22, significantly higher than the control group with an average CD31 protein fluorescence intensity of

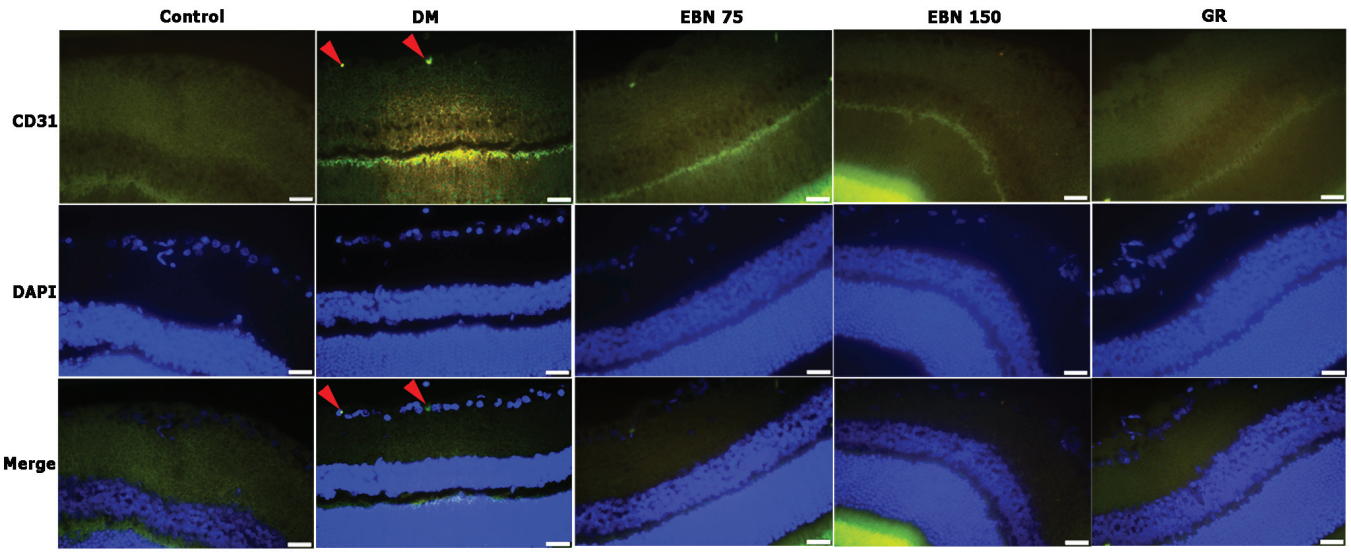

Fig. 4. Immunofluorescence micrographs of the CD31 protein expression within the retinal layers of the experimental rats across all 5 groups have been obtained. Notably, a prominent CD31 protein expression was observed along the vascular linings, particularly evident in the well-defined visualization within the vascular walls. Within the diabetes-induced experimental cohort (DM), a distinct VEGF protein expression was also apparent, as indicated by the red arrowheads. Scale bar: 20 μm.

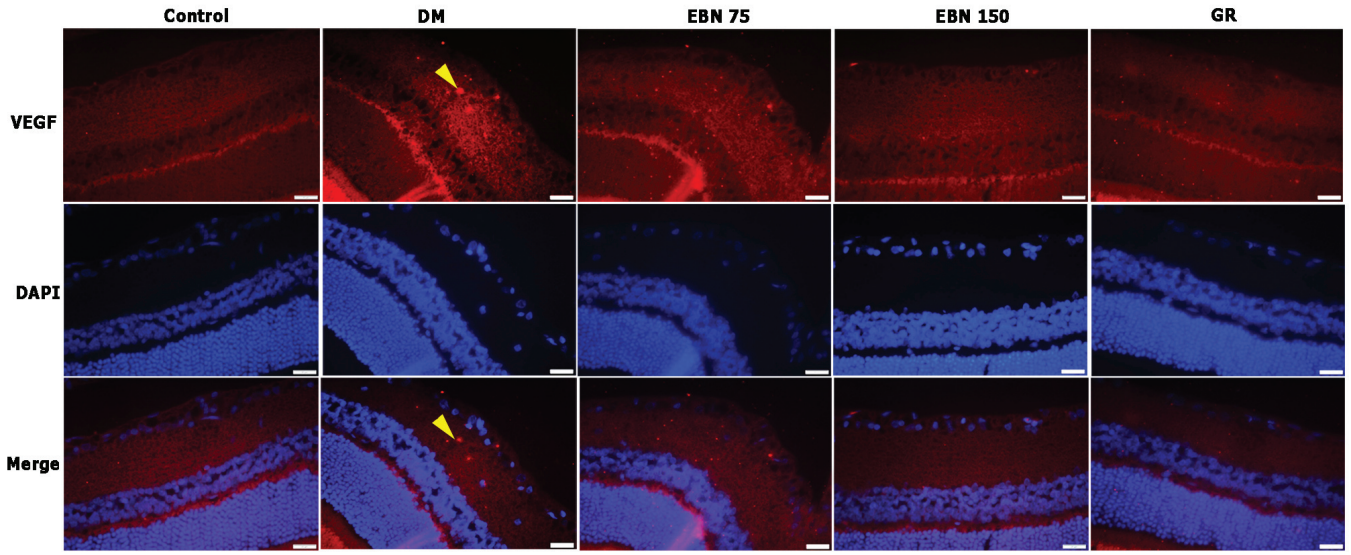

Fig. 5. Immunofluorescence micrographs depicting the expression of VEGF protein within the retinal layer in experimental mice from all five groups. Notably, within the ganglion cells layer of diabetes-induced (DM) rats, a distinct expression of VEGF protein is evident, as indicated by the yellow arrowheads. Scale bar: 20 μm.

14.42±0.64. Further examination of CD31 protein expression in experimental groups EBN75, EBN150, and GR (Fig. 4) revealed average fluorescence intensities of 26.10±0.59, 19.84±0.83, and 17.10±0.71, respectively. Notably, CD31 protein expression in the retinal layers showed a slight reduction in the EBN75 group and a statistically significant decrease in the EBN150 and GR groups compared with the DM group.

In the context of investigating the immunofluorescence-based protein expression of VEGF within the retinal ganglion cell layer and retinal vasculature wall, a comprehensive examination was conducted on experimental mice encompassing five distinct groups. Particularly noteworthy is the observed VEGF protein expression pattern within the retinal microenvironment of DM-induced mice as compared with the control group. Notably, a marked elevation in VEGF protein expression was evidenced in the ganglion cell layer and retinal vasculature of the DM group, substantiated visually in Figure 5. Quantitative evaluation of average VEGF fluorescence intensity within the DM cohort revealed a notable measurement of 30.51±2.62, signifying a discernible elevation when juxtaposed with the control group exhibiting a corresponding average measurement of 15.66±1.60. Furthermore, insights were garnered from the scrutiny of VEGF protein expression within experimental rats belonging to the EBN75, EBN150, and GR groups, as seen in Figure 5, with an intensity of 28.69±0.78, 21.77±1.17, and 18.02±1.45, respectively. It was noted that the expression of VEGF protein in the retinal tissue exhibited a slight decrease in group EBN75 and a statistically significant reduction in groups EBN150 and GR when compared with the DM group.

A PDGFR-β immunohistochemistry study of the retina in the different groups

Immunohistochemical analysis of the retinal layers revealed the expression of PDGFR-β at the Internal Limiting Membrane (ILM) in the DM group (Fig. 6B), displaying a significant upregulation compared with the control group (Fig. 6A). Conversely, a statistically significant downregulation was observed in the EBN75 (Fig. 6C), EBN150 (Fig. 6D), and GR (Fig. 6E) groups. The extent of reduction among these three groups showed a comparable trend. The mean Intensity of PDGFR-β, as quantified across all five groups, is shown in Figure 6F.

Vascular corrosion casting using SEM to study the retinal vasculature

In the control group, the retinal vasculature of

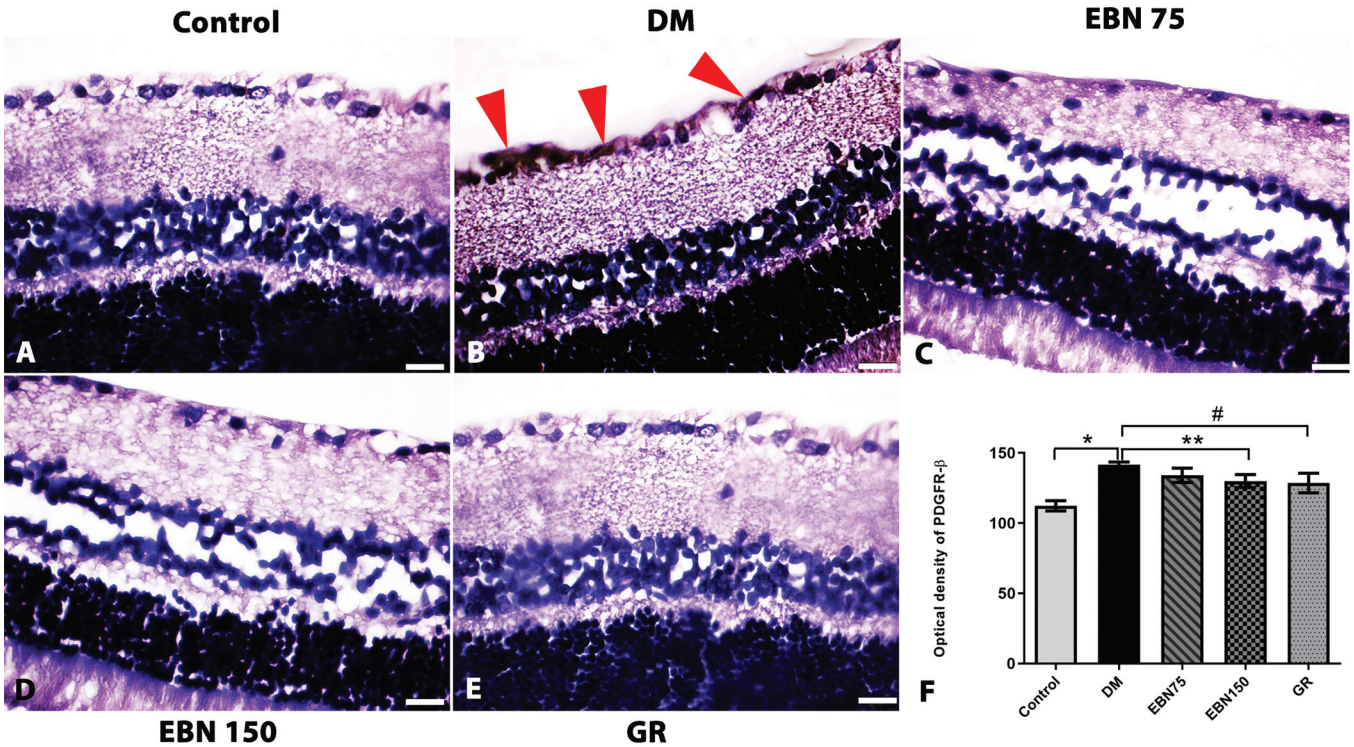

Fig. 6. Immunohistochemistry micrographs depicting the expression of PDGFR-β protein at the retinal layers in all five experimental groups (A-E) revealed pronounced expression at the Internal Limiting Membrane (ILM) in the DM group (red arrowheads). Comparative graph presentation of PDGFR-β protein expression in the retinal layer among all 5 experimental groups in rat. *p<0.0001 compared to group C. **p<0.01, #significantly different (p<0.01) compared to group DM. Scale bar: 20 μm.

experimental rats exhibited a well-organized and meticulously formed capillary plexus originating from the ophthalmic artery. This intricate network showcased an orderly alignment of capillaries with smooth vessel walls, devoid of any evident structural disruptions (Fig. 7A). The average diameter of retinal capillaries within the control group was quantified at 8.58±0.80 µm (Table 2). Conversely, in the DM group, induced diabetic rats displayed disorganized capillary plexus formation within the retinal layer. Irregularities and flattening of blood vessels were observed. The vessel walls exhibited irregular surfaces, and instances of capillary plexus fusion were observed, creating widened sheets (Fig. 7B), indicating the occurrence of compromised vascular integrity under diabetic conditions. The vessel walls were non-smooth, and the arrangement was irregular, potentially leading to impaired blood transportation. The average diameter of retinal capillaries in the DM group was significantly reduced (p<0.0001) compared with the control group, measuring 4.95±0.18 µm (Table 2).

In contrast, in the experimental groups treated with EBN75, EBN150, and GR (Fig. 7), a more regulated vasculature architecture was observed in the retina. The blood vessel arrangement exhibited enhanced organization, manifesting a more uniform arrangement and smoother vessel surfaces. However, in the EBN75 group, the fusion of the capillary plexus was noted (Fig. 7C). Meanwhile, the EBN150 and GR groups exhibited restored vessel tightness and diameter dimensions akin to the control group, signifying significant recovery ($^{\#}p$<0.1, $^{\#\#}p$<0.001, respectively) relative to the DM group (Table 2).

Table 2. Diameter of retinal capillaries plexus (μm) in each distinct experimental rat group.

Groups	Diameter of retinal capillaries plexus (μm)
Control	8.58±0.80
DM	4.95±0.18*
EBN75	5.36±0.146$^{\#\#}$
EBN150	7.10± 0.44$^{\#\#}$
GR	8.35±0.44$^{\#}$

Data are presented as mean ± SEM, *p<0.001 compared with the control group, $^{\#}p$<0.001, $^{\#\#}p$<0.1 compared with the DM group.

Discussion

This study of DM in experimental rat groups revealed distinct diabetic conditions in each group. Rats in the DM group exhibited hyperglycemia, indicated by blood glucose levels ≥ 250 mg/dl, along with symptoms of polydipsia (excessive thirst), polyuria (increased urination), and polyphagia (excessive hunger). When comparing this group with the DM group administered EBN, a significant reduction in blood glucose levels was observed in the latter. This finding aligns with the research conducted by Murugan (Murugan et al., 2020), who observed a reduction in blood glucose levels in db/db male rats after a four-week experimental period following hydrolyzed bird's nest (HBN) administration.

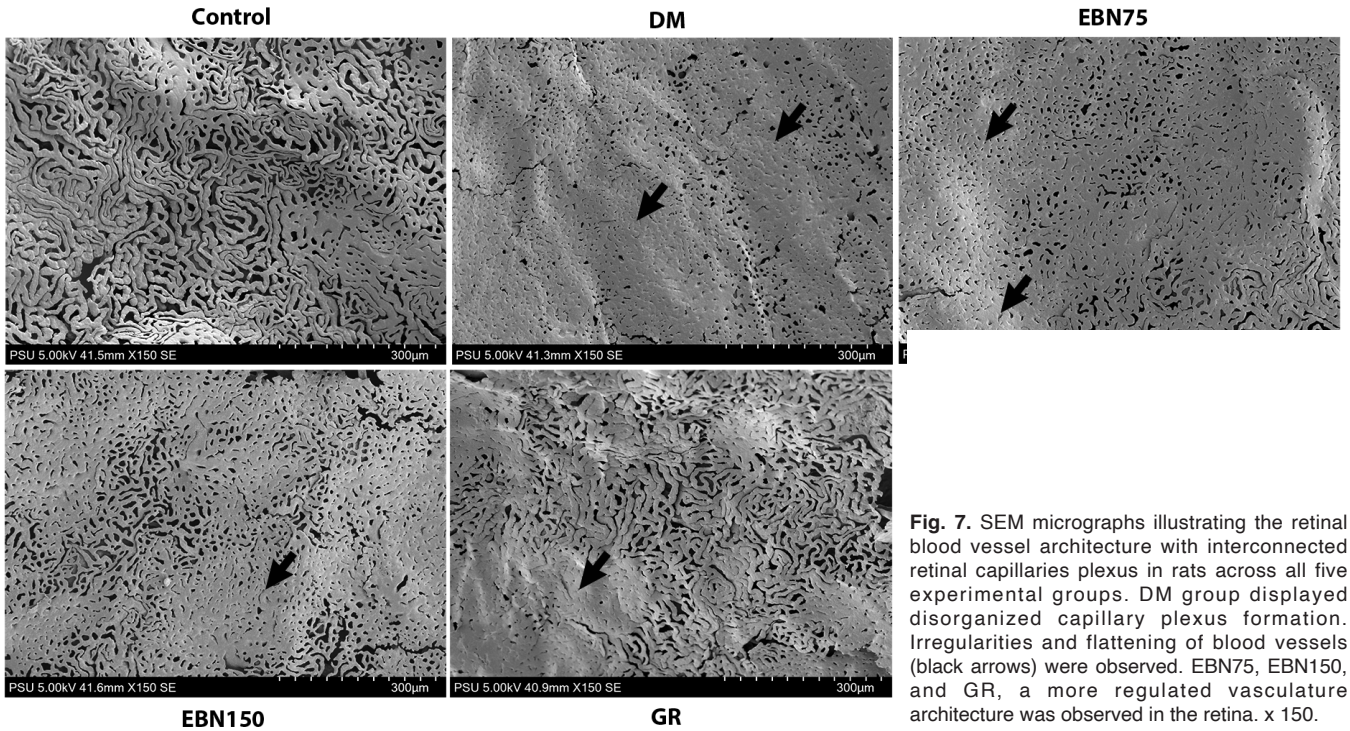

Fig. 7. SEM micrographs illustrating the retinal blood vessel architecture with interconnected retinal capillaries plexus in rats across all five experimental groups. DM group displayed disorganized capillary plexus formation. Irregularities and flattening of blood vessels (black arrows) were observed. EBN75, EBN150, and GR, a more regulated vasculature architecture was observed in the retina. x 150.

The blood glucose level reduction attributed to HBN stemmed from its ability to reduce reactive oxygen species markers, such as NOX-2 and nitrotyrosine, while concurrently enhancing the expression of SOD-1 and phosphorylated eNOS in endothelial cells within the aorta of db/db rats.

The escalation of free radical production due to hyperglycemia leads to the generation of advanced glycosylated end-products (AGEs) and subsequent alterations in vascular permeability. This results in the thickening of the basement membrane and collagen accumulation, impacting blood vessel flexibility. The modulation of eNOS and guanylyl cyclase, as well as the involvement of PKC-β and its downstream signaling molecules, further contribute to diminished nitric oxide responsiveness. This cascade of events underscores the intricate interplay between hyperglycemia-induced pathways, highlighting the need for interventions to rectify the imbalanced NO and ROS levels associated with vascular dysfunction in DM (Murugan et al., 2020). By controlling the ROS pathway, HBN can restore endothelial function and protect endothelial cells from oxidative damage caused by high glucose in Human Umbilical Vein Endothelial Cells (HUVECs), isolated mouse aorta, and db/db diabetic mice. This ultimately increases the bioavailability of NO. Furthermore, these data suggest that HBN may play a role in the maintenance of endothelial function as well as the management of microvascular or macrovascular problems in DM patients (Murugan et al., 2020).

The elevated blood glucose levels observed in this study induced detrimental effects on retinal blood vessels, affecting both large vessels, such as the ophthalmic artery, and smaller vessels at the capillary level. Notably, the most pronounced damage was observed in the smallest vessels, specifically the capillaries, which exhibited fusion and shrinkage. This microvascular damage could potentially lead to reduced blood flow to the retina. Additionally, medium-sized arterioles and larger arteries displayed signs of constriction, indicating compromised blood vessel function. The vessel walls exhibited irregularities, impacting proper blood transportation. In some instances, angiogenesis, characterized by sprouting of new blood vessels, was noted in the DM rat group. This process aimed to ensure adequate blood supply to retinal tissues. Key growth factors involved in angiogenesis include VEGF and transforming growth factor-Beta (TGF-β) (Chen et al., 2020). CD31 is an endothelial cell marker that may identify angiogenesis in atherosclerosis. Every single protein domain found in CD31 plays distinct roles in the cells as well as in the progression of vascular and other inflammatory disease (Liu and Shi, 2012). To facilitate the growth of supporting cells within the vasculature, PDGFR-β is an indispensable factor. The PDGFR-β pathway functions as an upstream regulator that is activated following the retinal ischemia-reperfusion that damages the retinal microvascular system (Li et al., 2023). PDGFR-β overexpression is responsible for the proliferation and angiogenesis that occur in the endothelial cell model. Additionally, the loss of retinal ganglion cells that occurs in the rat retinal ischemia-reperfusion model is a result of this upregulation (Li et al., 2023). There is a possibility that the increased production of PDGF-β in the retina could result in the creation of an epiretinal membrane and traction retinal separation. This is a significant characteristic of the proliferative phase of DR (Cao et al., 2023). These factors were found to play pivotal roles in driving neovascularization. From prior research, it is evident that prolonged hyperglycemia triggers changes in retinal microvasculature, resulting in capillary occlusion and compromising blood-retinal barrier integrity. Accompanying hypertension in DM patients contributes to arterial stiffness, thickening vessel walls, and further constriction, aggravating ocular complications.

Treatment with 150 mg/kg BW of EBN extract exhibited positive effects on retinal blood vessels. In addition to the biomarker chemicals, sialic acid, HBN was provisionally found. HBN was used to identify three distinct kinds of sialic acid, known as N-acetylmuramic acid, N-acetylneuraminic acid, and N-acetyl-2,7-anhydro-alpha-neuraminic acid (Choy et al., 2021). In arterioles and larger arteries, the inner vessel wall showed improvements, leading to reduced constriction. This might be attributed to the extract's antioxidative and anti-inflammatory properties. Furthermore, the treatment seemed to modulate key signaling pathways, inflammatory factors, and growth factors pivotal in DM pathogenesis.

Immunohistochemical analysis comparing protein expression of VEGF, CD31, and PDGFR-β revealed significant increases in the DM group compared with the control, particularly under conditions of retinal hypoxia induced by oxidative stress and inflammation. This phenomenon triggered hypoxia-inducible factor 1 (HIF-1) production, driving the elevation of TGF-β and VEGF. Simultaneously, diabetes-induced retinal hypoxia seemed to damage Müller cells, leading to increased release of glial fibrillary acidic protein (GFAP) and further upregulation of VEGF, supporting angiogenesis (Aiello and Wong, 2000).

Inflammation is reduced, and the retinal tissue is protected against hyperglycemic insults because of the significant reduction in VEGF, CD31, and PDGFR-β associated with supplementation with 150 mg/kg of HBN. Experiments conducted on β-Cell function and insulin signaling in Type 2 DM Mice indicated that EBN possesses comparable anti-inflammatory and antioxidant properties (Choy et al., 2021). Upon treatment with EBN extract, protein levels of VEGF, CD31, and PDGFR-β exhibited statistically significant reductions compared with the DM group. This reduction could be attributed to the extract's anti-inflammatory and antioxidative effects. The extract's efficacy in dampening these factors could potentially contribute to inhibiting angiogenesis by reducing inflammation and oxidative stress.

Conclusion

The present study demonstrated that treatment with 150 mg/kg BW of EBN extract effectively lowers blood glucose levels and mitigates the increased expression of VEGF, CD31, and PDGFR-β. These findings suggest a potential role in preventing neovascularization, extracellular matrix accumulation, and associated retinal pathologies induced by diabetes.

Acknowledgements. This research was supported by the National Science, Research, and Innovation Fund (NSRF) and Prince of Songkla University (Grant No AGR6505062M), Thailand.

Declaration of Competing Interest. The authors declare that none of the work reported in this study could have been influenced by any known competing financial interests or personal relationships.

Data availability. Data will be made available on request.

References

Aiello L.P. and Wong J.-S. (2000). Role of vascular endothelial growth factor in diabetic vascular complications. Kidney Int. Suppl. 58, S113-119.

Brownlee M. (2005). The pathobiology of diabetic complications: A unifying mechanism. Diabetes 54, 1615-1625.

Cao Z., Liu Y., Wang Y. and Leng P. (2023). Research progress on the role of PDGF/PDGFR in type 2 diabetes. Biomed. Pharmacother. 164, 114983.

Careena S., Sani D., Tan S.N., Lim C.W., Hassan S., Norhafizah M., Kirby B.P., Ideris A., Stanslas J., Basri H.B. and Lim C.T. (2018). Effect of edible bird's nest extract on lipopolysaccharide-induced impairment of learning and memory in Wistar rats. Evid. Based Complement. Alternat. Med. 2018, 9318789.

Chen H.Y., Ho Y.J., Chou H.C., Liao E.C., Tsai Y.T., Wei Y.S., Lin L.H., Lin M.-W., Wang Y.-S., Ko M.-L. and Chan H.-L. (2020). The role of transforming growth factor-beta in retinal ganglion cells with hyperglycemia and oxidative stress. Int. J. Mol. Sci. 21, 1-21.

Choy K.W., Md Zain Z., Murugan D.D., Giribabu N., Zamakshshari N.H., Lim Y.M. and Mustafa, M.R. (2021). Effect of hydrolyzed bird's nest on β-cell function and insulin signaling in type 2 diabetic mice. Front. Pharmacol. 12, 632169.

Guo S., Tian H., Dong R., Yang N., Zhang Y., Yao S., Li Y., Zhou Y., Si Y. and Qin S. (2016). Exogenous supplement of N-acetylneuraminic acid ameliorates atherosclerosis in apolipoprotein E-deficient mice. Atherosclerosis 251, 183-191.

Haghani A., Mehrbod P., Safi N., Aminuddin N.A., Bahadoran A., Omar A.R. and Ideris A. (2016). *In vitro* and *in vivo* mechanism of immunomodulatory and antiviral activity of edible bird's nest (EBN) against influenza A virus (IAV) infection. J. Ethnopharmacol. 185, 327-340.

Klein B.E.K. (2007). Overview of epidemiologic studies of diabetic retinopathy. Ophthalmic Epidemiol. 14, 179-183.

Komolkriengkrai M., Nopparat J., Vongvatcharanon U., Anupunpisit V. and Khimmaktong W. (2019). Effect of glabridin on collagen deposition in liver and amelioration of hepatocyte destruction in diabetes rats. Exp. Ther. Med. 18, 1164-1174.

Li J., Chen C., Zhang L., Ren Y. and Li H. (2023). PDGFRB upregulation contributes to retinal damages in the rat model of retinal ischemia-reperfusion. Biochem. Biophys. Res. Commun. 663, 113-121.

Liu L. and Shi G.P. (2012). CD31: Beyond a marker for endothelial cells. Cardiovasc. Res. 94, 3-5.

Ma, F., and Liu, D. (2012). Sketch of the edible bird's nest and its important bioactivities. Food Res. Int. 48, 559-567.

Murugan D.D., Md Zain Z., Choy K.W., Zamakshshari N.H., Choong M.J., Lim Y.M. and Mustafa M.R. (2020). Edible bird's nest protects against hyperglycemia-induced oxidative stress and endothelial dysfunction. Front. Pharmacol. 10, 1624.

Oliveros E., Vázquez E., Barranco A., Ramírez M., Gruart A., Delgado-García J.M., Buck R., Rueda R. and Martín M.J. (2018). Sialic acid and sialylated oligosaccharide supplementation during lactation improves learning and memory in rats. Nutrients 10, 1519.

Park Y.G. and Roh Y.J. (2016). New diagnostic and therapeutic approaches for preventing the progression of diabetic retinopathy. J. Diabetes Res. 2016, 1753584.

Pitocco D., Zaccardi F., Di Stasio E., Romitelli F., Santini S.A., Zuppi C. and Ghirlanda G. (2010). Oxidative stress, nitric oxide, and diabetes. Rev. Diabet. Stud. 7, 15-25.

Roden M. (2016). Diabetes mellitus: Definition, classification and diagnose. Wien. Klin. Wochenschr. 128, 37-40 (in German).

Wang W. and Lo A.C.Y. (2018). Diabetic retinopathy: Pathophysiology and treatments. Int. J. Mol. Sci. 19, 1816.

Wu F., Jin Z. and Jin J. (2013). Hypoglycemic effects of glabridin, a polyphenolic flavonoid from licorice, in an animal model of diabetes mellitus. Mol. Med. Rep. 7, 1278-1282.

Yew M.Y., Koh R.Y., Chye S.M., Othman I. and Ng K.Y. (2014). Edible bird's nest ameliorates oxidative stress-induced apoptosis in SH-SY5Y human neuroblastoma cells. BMC Complement. Altern. Med. 14, 391.

Accepted October 1, 2024